

Large-Scale Spatio-Temporal Person Re-identification: Algorithm and Benchmark

Xiujun Shu[†], Xiao Wang[†], Shiliang Zhang, Xianghao Zhang, Yuanqi Chen, Ge Li*, and Qi Tian

Abstract—Person re-identification (re-ID) in the scenario with large spatial and temporal spans has not been fully explored. This is partially because that, existing benchmark datasets were mainly collected with limited spatial and temporal ranges, *e.g.*, using videos recorded in a few days by cameras in a specific region of the campus. Such limited spatial and temporal ranges make it hard to simulate the difficulties of person re-ID in real scenarios. In this work, we contribute a novel Large-scale Spatio-Temporal (LaST) person re-ID dataset, including 10,860 identities with more than 224k images. Compared with existing datasets, LaST presents more challenging and high-diversity re-ID settings, and significantly larger spatial and temporal ranges. For instance, each person can appear in different cities or countries, and in various time slots from daytime to night, and in different seasons from spring to winter. To our best knowledge, LaST is a novel person re-ID dataset with the largest spatio-temporal ranges. Based on LaST, we verified its challenge by conducting a comprehensive performance evaluation of 14 re-ID algorithms. We further propose an easy-to-implement baseline that works well on such challenging re-ID setting. We also verified that models pre-trained on LaST can generalize well on existing datasets with short-term and cloth-changing scenarios. We expect LaST to inspire future works toward more realistic and challenging re-ID tasks. More information about the dataset is available at <https://github.com/shuxjweb/last.git>.

Index Terms—Person Re-identification, Person Retrieval, Person Recognition, Benchmark.

I. INTRODUCTION

PERSON re-identification (re-ID), as a sub-task of image retrieval [1, 2], aims to match the same person in non-overlapping cameras [3]. Existing benchmarks focus on short-term person re-ID task, *e.g.*, CUHK03 [4], Market1501 [5], and DukeMTMC [6], have played important roles in promoting re-ID research in recent years. However, performance on these benchmarks is becoming saturated, *e.g.*, the Rank1 accuracy exceeds 96% on Market1501. Notwithstanding their remarkable success on those datasets, current person re-ID algorithms still exhibit limitations in real applications, where the query person may appear at different locations and wear different clothes. Therefore, it still exists a large gap between these benchmark datasets and practical applications.

[†]Equal Contribution. *Corresponding author.(e-mail: geli@ece.pku.edu.cn)
Xiujun Shu is with Peng Cheng Laboratory and Peking University, Shenzhen, China.(e-mail: shuxj@pcl.ac.cn)

Xiao Wang is with Peng Cheng Laboratory, Shenzhen, China. (e-mail: wangx03@pcl.ac.cn)

Ge Li, Xianghao Zang and Yuanqi Chen are with School of Electronic and Computer Engineering, Peking University, Shenzhen, China. (e-mail: geli@ece.pku.edu.cn, zangxh@pku.edu.cn, cyq373@pku.edu.cn)

Shiliang Zhang is with School of Electronic Engineering and Computer Science, Peking University, Beijing, China. (e-mail: slzhang.jdl@pku.edu.cn)

Qi Tian is with the Huawei Cloud & AI, Huawei Technologies, China. (e-mail: tian.qi1@huawei.com)

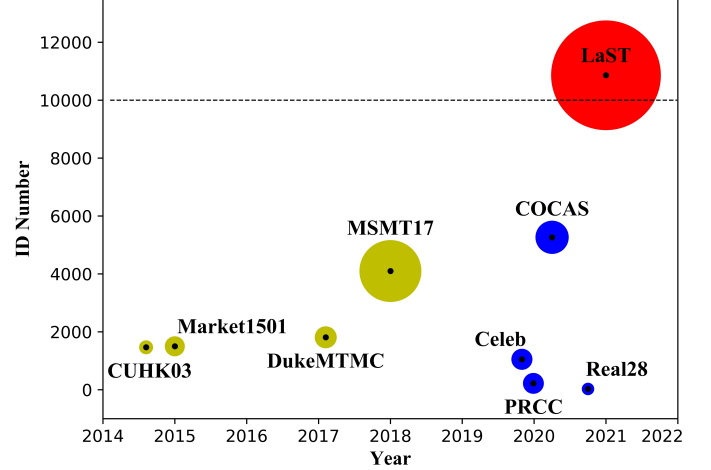


Fig. 1. Summaries of densely annotated re-ID benchmarks. The vertical axis represents the number of identities and the circle diameter is in proportion to the number of images. The yellow cycles are conventional re-ID benchmark datasets. The blue circles are cloth-changing datasets.

According to our observation, there are two gaps between conventional benchmarks and real scenarios. **First**, the spatial scope of pedestrian activities is small. Most existing benchmarks were collected in a local region of the campus. The spatial scope is relatively small. This is quite different from the setting of real-world scenarios. For example, a suspect commonly need to be searched across cameras in several districts or the entire city. **Second**, the time span of pedestrian activities is short. Most of existing re-ID datasets define a short-term re-ID task, where the weather and clothes stay stable. This simplified setting also differs with the real one, where the suspects may appear at both daytime and night, and change clothes. The two gaps hinder the further development of person re-identification.

To address this issue, some searchers have released several cloth-changing datasets recently, *e.g.*, PRCC [7], COCAS [8] and Real28 [9]. However, those datasets are small in scale, and also only cover a limited spatial regions. For example, the Real28 [9] dataset only collects images of 28 persons, the PRCC [7] are captured in the indoor environment, and the pedestrian images of COCAS [8] dataset only last for four days. These limitations make them hard to simulate real-world scenarios for person re-ID. The re-ID community urgently needs a larger and more challenging dataset.

In this work, we study a more realistic person re-ID setting, which presents larger spatial and temporal ranges. We contribute a large-scale benchmark, named **LaST**, which contains

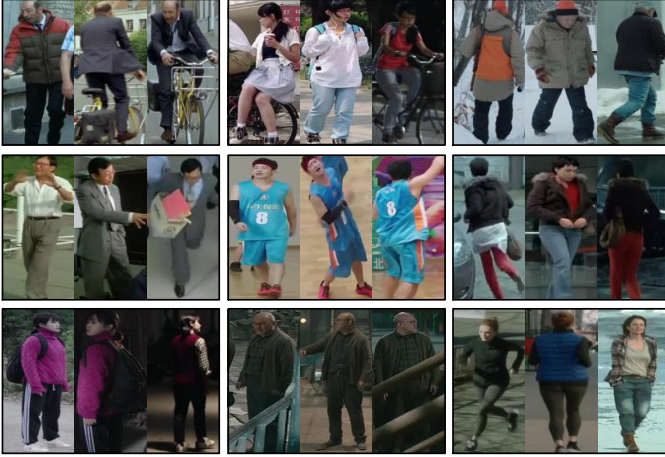


Fig. 2. **Sample images of the LaST dataset.** Nine persons are shown and each person has three instances.

10,860 identities with 224,721 images. As shown in Fig. 1, this is the first densely annotated re-ID benchmark with more than 10k identities. Creating a large-scale person re-ID dataset covering long-range spatial and temporal spans is challenging, for both video collection and data annotation. To make this procedure feasible, we explored a novel strategy by utilizing movies, which contain plenty of person images. Specifically, LaST is collected from detected persons in 2k movies. As most movies contain realistic scenes and characters, LaST is a valid benchmark for person re-ID algorithms. Moreover, compared with previous dataset construction methods, our strategy demonstrates the following advantages:

- **Privacy Protection.** Using persons detected in movies is superior to previous methods in privacy protection, which is increasingly important nowadays.
- **Diversity.** As shown in Fig. 2, scenes in movies are diverse, *e.g.*, contain both indoor, outdoor scenes. The same person can appear in different cities, counties, and wear various clothes.
- **Annotations.** Annotating persons in each movie is easier than the annotation in large-scale surveillance videos. This property ensures a budget-aware dataset construction.

Although LaST comes from movies, its style is very similar to existing datasets. This is because eight labelers are involved to select images that have similar viewpoints to real surveillance scenes. The state-of-the-art methods were evaluated on LaST and results show that LaST is more challenging than existing reid benchmarks. We further propose an efficient baseline that works well on LaST. Specifically, it treats re-ID as a retrieval task, and directly optimizes the retrieval mAP during training. Compared with previous works, that commonly use triplet loss [10] or cross-entropy loss for training, our method achieves competitive performance compared with the state-of-the-art methods. We also propose a pre-training strategy based on LaST. Extensive experiments show that, pre-trained model on LaST demonstrates superior generalization ability on existing datasets, *i.e.*, both the short-term datasets and those cloth-changing ones.

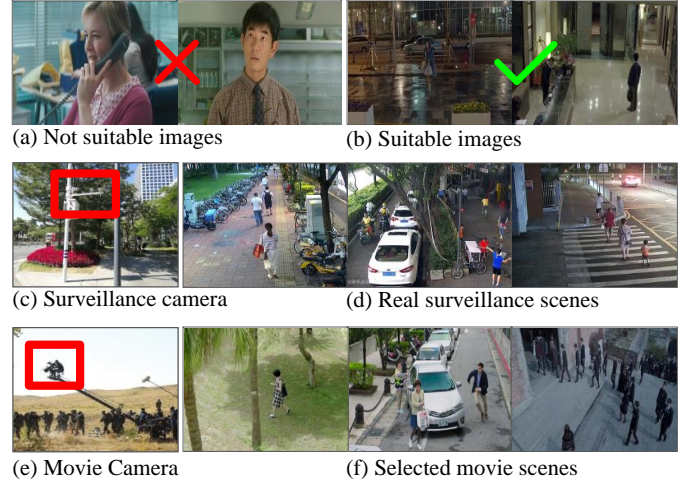


Fig. 3. **Comparison of movie scenes and surveillance scenes.**

In summary, our contributions are three-fold: **(1)** We contribute a large-scale benchmark dataset named **LaST** for person re-ID. It consists of 10,860 identities and 224,721 images in total. LaST is highly diverse capturing from a broad range of countries, person ages, scenes, weather, daytime and night. Besides, it is the first one to label clothes to date. **(2)** We propose an efficient baseline approach that works well on such challenging person re-ID setting. We also report the results of 14 recent person re-ID algorithms based on LaST for future works to compare. **(3)** We conduct extensive experiments to verify the generalization ability of LaST on other re-ID datasets.

II. RELATED WORK

A. Short-Term Re-ID Benchmarks

Most re-ID benchmarks have contributed to this field in different stages. In early stages, GRID [11] contains 1,025 and 1,275 images captured by eight disjoint cameras in a busy underground station. CUHK01 [12] was collected on campus, which contains 971 identities and 3,884 images. The short-coming of these datasets is that the quantity of images is too small. In later years, several larger datasets, *e.g.*, CUHK03[4], Market1501[5], DukeMTMC[6], and MSMT17 [13], have been popularly studied in the re-ID community. Market1501[5] was collected in Tsinghua University. It has 1,501 identities and 31,466 images in total. DukeMTMC [13] was collected in Duke University. It contains 1,812 identities and 36,411 images. As these dataset were collected in campus, most pedestrians are colleague students or faculties. Besides, the performance on these datasets is becoming saturated to date. For example, the Rank1 value exceeds 96% on Market1501 and reaches 91.6% on DukeMTMC. Besides, all these datasets focus on local space and short-term settings. They assume that the clothes of pedestrians would not change significantly. This assumption has a certain gap with real scenes and would limit the application in real-world scenarios.

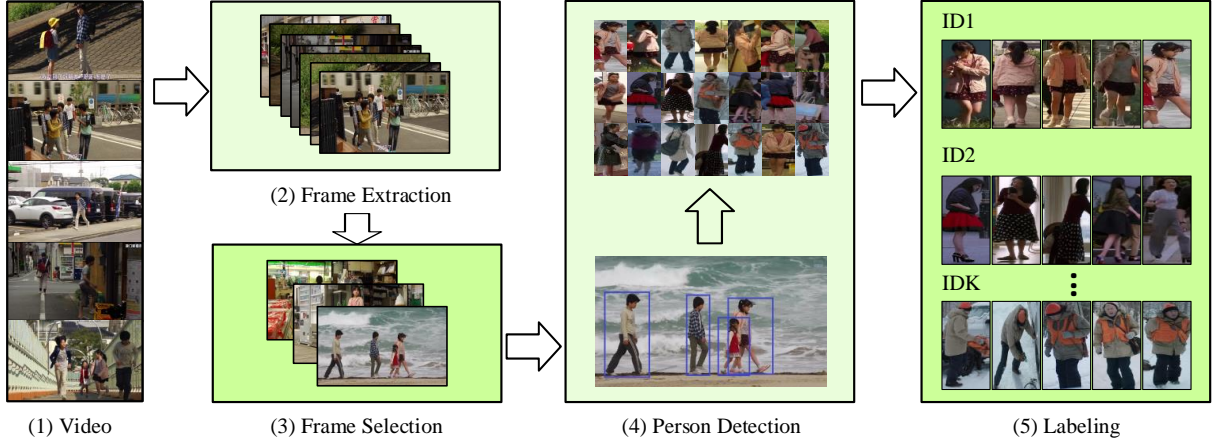


Fig. 4. **The pipeline of data building.** The second and fourth steps are processed by PLabel. The third and fifth steps require human participation. Finally, the PLabel automatically records the results of manual annotation.

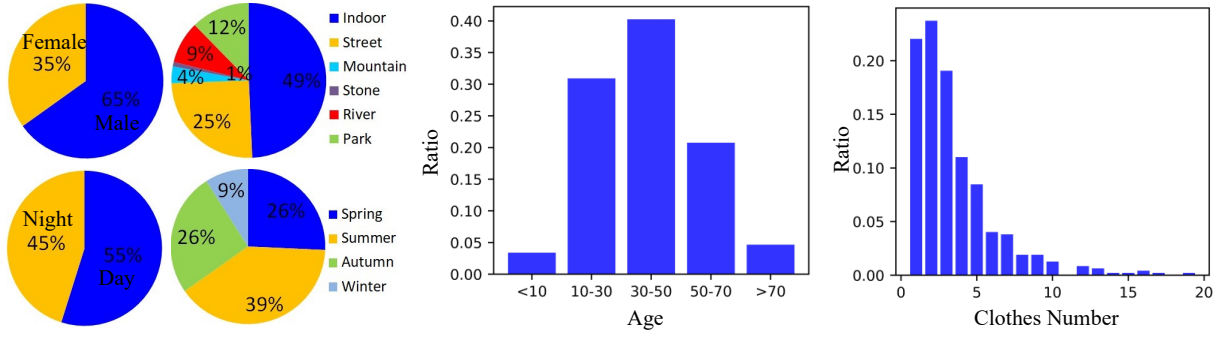


Fig. 5. **Statistical information of LaST.** All the information was counted by labelers. The ages were estimated. The stone denotes the area full of sand or stones.

B. Cloth-Changing Re-ID Benchmarks

Recently, some scholars in this field have made some efforts on the long-term re-ID and released several cloth-changing datasets. They assume that the query and the gallery of the same identity have different clothes. PRCC [7] includes 221 identities and 33,698 images, which capture several students in the teaching room. This dataset aims to exploit the contour sketch in the cloth-changing scenario. COCAS [8] contains 5,266 identities and 62,384 images. It uses a cloth-template as a reference to retrieve the target person. This setting reduces the difficulty of cloth-changing person re-ID. Real28 is a small-scale benchmark consisting of 28 identities and 4,324 images. LTCC [14] contains 152 identities and 17,138 images. The above datasets mainly focus on the cloth-changing issue in the time dimension. The activity scopes of pedestrians in space are limited because only a few people are recruited. Besides, the sizes of these datasets are still small.

C. Spatio-Temporal Re-ID Benchmarks

There are several related datasets from photo albums, short videos or movies to date. PIPA [15] contains 2,356 identities, which was collected from public photo albums. CIP [15] contains 4,204 identities, which was collected from the Internet. CIM [16] consists of 1,218 identities, which was collected from movies. However, the pedestrians in these datasets are not

cropped images, but in the “wild”. They were designed not for person re-ID, but for person retrieval or person search. CUHK-SYSU [17] is used for person search, which was collected by hand-held cameras and snapshots from movies. Celeb-reID [18] contains 1,052 identities, which was acquired from the Internet using street snap-shots of celebrities. This is the most similar dataset to ours, but still significantly different from ours. Its shortcoming is that most pedestrians are on the frontal view. Also, the light is always bright and lacks diversity. In contrast, LaST only selects the images with view angles similar to surveillance scenes. The variations in pedestrian pose, illumination, and scenes are quite diverse. Besides, the identity number of LaST is much larger than Celeb-reID.

III. BENCHMARK BUILDING AND STATISTICS

LaST aims to offer the community a large-scale benchmark covering long-range spatial and temporal spans. It was collected from movies and built by a self-developed semi-automatic annotation tool called PLabel, which had been open-sourced¹. More details about dataset building and statistics are shown as follows.

A. Dataset Building

Due to privacy protection, it is difficult to obtain regional or city level monitoring data in reality. Therefore, most current re-

¹<https://code.iHub.org.cn/projects/4420>

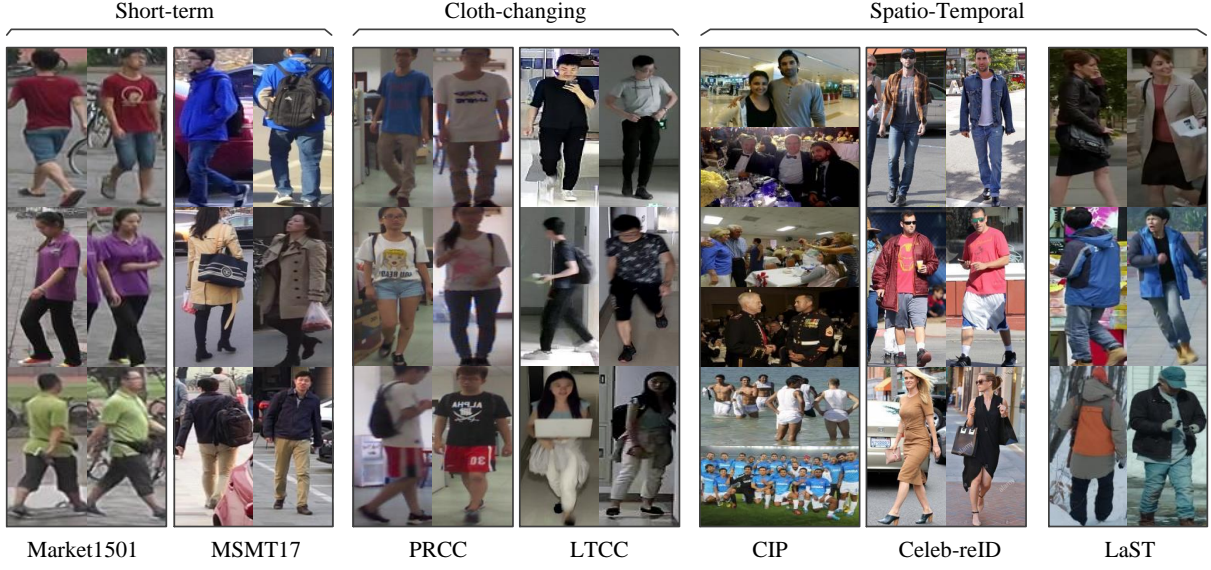


Fig. 6. **The style comparison of different benchmarks.** Market1501 and MSMT17 were collected on campus. PRCC and LTCC were collected indoors. CIP and Celeb-reID were acquired from the Internet.



Fig. 7. **The illustration of clothing labels.** Each row denotes the same person. A_B denotes the labels, in which A is the identity label and B is the clothing label. The little girl in the first row does not change her clothes. All the clothing labels are 01. The man in the second row has a total of 3 suits. The girl in the third row has eight clothes.

ID benchmarks were collected in local space by recruiting few people. Movies are good material for making re-ID datasets due to several reasons, *e.g.*, real pedestrians, diverse scenes, rich poses, and illumination changes. Besides, persons in movies move around with a wide scope and a long-time span.

However, most images in movies are not suitable because only the head or upper body can be seen (see Fig. 3(a)). Therefore, we carefully select images that cover most of bodies and have similar view angles to surveillance scenes (see Fig. 3(b)). This is the biggest difference between LaST and other Internet-based datasets. As shown in Fig. 3(c), most surveillance cameras are installed at a height of 3 to 5 meters.

In movies, some cameras using high angle shot have similar heights (see Fig. 3(e)). As shown in Fig. 3(d) and (f), the selected movie scenes are similar to real surveillance scenes. We also noticed that some movies will be post-processed, which leads to the changes of color and illumination to some extent. This operation can be regarded as the data augmentation. We have verified the generalization ability of LaST in the following experiments.

To ensure diversity, we collected more than 2k movies, covering more than 8 countries from Asia to Europe. We recruited eight labelers to complete the annotation work for 2.5 months. All the annotations were done using our developed

TABLE I
COMPARISON OF LAST WITH PREVIOUS RE-ID BENCHMARKS. “CROP” MEANS DETECTED BOUNDING BOX. “BODY” MEANS SIMILAR VIEW ANGLES TO SURVEILLANCE SCENES AND THE WHOLE BODY CAN BE SEEN. “TIME” MEANS LONG-TERM. “SPACE” MEANS LARGE ACTIVITY SCOPE. “CLOTHING ID” IS THE LABEL OF CLOTHES.

Dataset	Year	ID Num	Images	Cameras	Crop	Body	Time	Space	Clothing ID
VIPeR[19]	2007	632	1,264	2	✓				
GRID[11]	2009	1,025	1,275	8	✓				
CUHK01[12]	2012	971	3,884	2	✓	✓			
CUHK03[4]	2014	1,467	13,164	10	✓	✓			
Market1501[5]	2015	1,501	31,466	6	✓	✓			
DukeMTMC[6]	2017	1,812	36,411	8	✓	✓			
MSMT17[13]	2018	4,101	124,068	6	✓	✓			
PIPA[15]	2015	2,356	37,107	*	✓		✓	✓	
CIP[15]	2016	4,204	37,916	*	✓		✓	✓	
CIM[16]	2018	1,218	72,875	*	✓		✓	✓	
Celeb-reID[20]	2019	1,052	34,186	*	✓	✓	✓	✓	
PRCC[7]	2020	221	33,698	3	✓	✓	✓		
COCAS[8]	2020	5,266	62,382	30	✓	✓	✓		
Real28[9]	2020	28	4,324	4	✓	✓	✓		
LTCC[14]	2020	152	17,138	12	✓	✓	✓		
LaST	2021	10,860	224,721	*	✓	✓	✓	✓	✓

tool called PLabel. The pipeline of data building is shown in Fig. 4. First, the frames were extracted by PLabel. To reduce redundancy, the frames were then selected every several seconds. Besides, we keep only one frame in each scene or perspective. In this way, it can be considered that each frame is captured by a different camera. Next, the PLabel detected persons [21] and marked the bounding boxes. Finally, we give each bounding box an ID number. The same person is assigned the same ID. The detected bounding boxes will be manually adjusted if the labelers observe substantial detection errors. After that, persons with less than five images were removed.

B. Statistical Characteristics

Fig. 5 gives some statistical characteristics. All the information was collected manually. Among the pedestrians, 65% are male and 35% are female. Many of them move among cities and even countries. We roughly divide the activity scenes into six categories: indoor, street, mountain, stone, river, and park. The stone denotes the area full of sand or stones. The river means a place where there is water, *e.g.*, river, lake, pool, beach. The large time span brings about two changes: clothes and the weather, *e.g.*, daytime and night, changing seasons. As shown in Fig. 5, it accounts for 55% during the daytime and 45% at night. The season covers from spring to winter. For pedestrians, the age span ranges from children to older people over 70 years old. 76% of them have changed their clothes. The maximum number for each person attains to 24.

C. Style comparison

Fig. 6 compares the style of different benchmarks. As Market1501[5] and MSMT17[13] were collected on campus, most pedestrians were college students or faculties. Most of the scenes are the streets and teaching buildings inside the

campus. PRCC[7] and LTCC[14] were collected by recruiting a few students to take pictures. Most scenes are indoors and the diversity of scenes is limited. CIP[15] and Celeb-reID[20] were acquired from the Internet, *e.g.*, YouTube and short videos. The samples in CIP are not cropped, so CIP is used for the task of person retrieval or person search. Celeb-reID[20] is from the street snap-shots of celebrities and most of the scenes are streets. LaST also belongs to spatio-temporal dataset and was collected from thousands of movies. As shown in Fig. 6, its style is similar to other real-scene datasets. Since movies are long videos, pedestrians in LaST have a larger space and time span. The scenes and clothing style in LaST are much more diverse.

D. Quantitative comparison

Table I gives some comparisons with existing datasets. LaST has 10,860 identities and 224,721 images, which are both larger than those of other datasets. Compared with short-term datasets, *e.g.*, CUHK03 [4] and Market1501[5], LaST is larger in scale and covers more complicated scenes. Compared with cloth-changing datasets, *e.g.*, PRCC[7] and COCAS[8], LaST has much more scenes. The changes of clothes and weather are still more diverse in LaST. Compared with other datasets, *e.g.*, PIPA[15], CIP[15], and CIM[16], LaST follows the popular person re-ID setting and provides cropped person images covering more complete person body. Besides, many images can only see the heads in these datasets. Celeb-reID is similar to LaST, but most images in Celeb-reID are taken from the frontal view and are bright in the daytime. LaST is more diverse in view angles and light changes than Celeb-reID. Besides, we labeled the clothing ID in LaST. As shown in Fig 7, we labeled the clothes for each person. Some persons do not change clothes, but some change clothes frequently. To

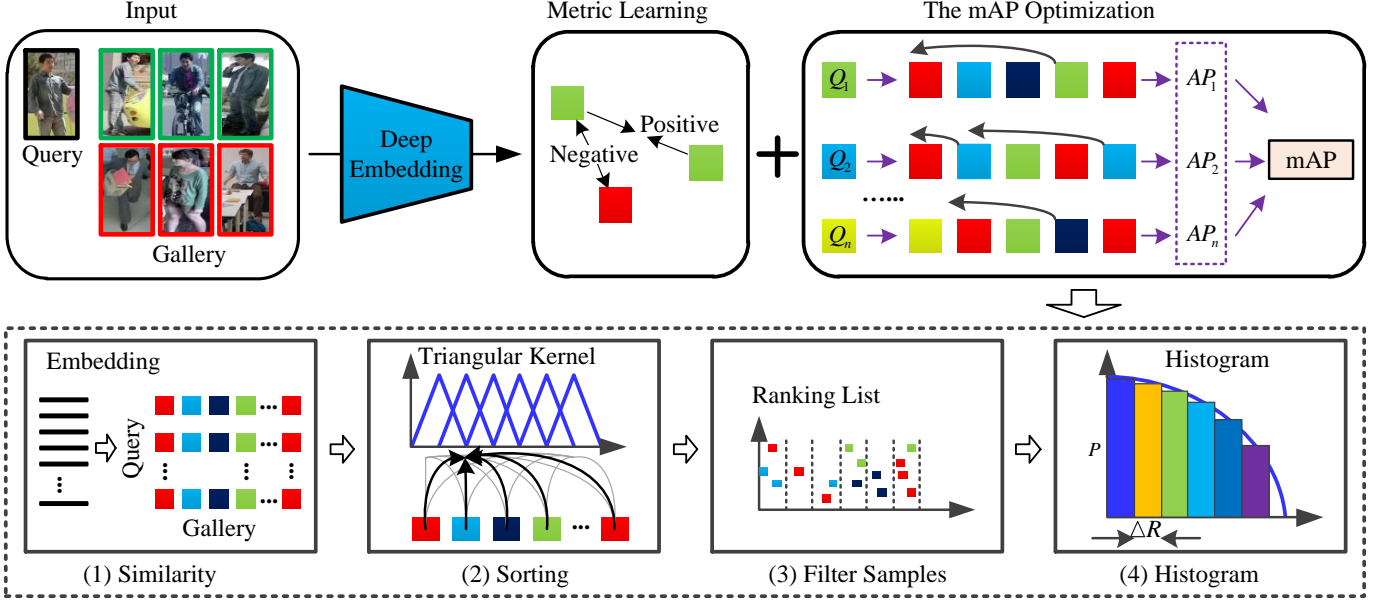


Fig. 8. **The flowchart of our approach.** Metric learning utilizes triplet loss to optimize the model. This is the same with existing re-ID methods. The mAP optimization utilizes histogram approximation to directly optimize the mAP accuracy.

the best of our knowledge, LaST is currently the first person re-ID dataset providing clothing labels.

IV. METHODOLOGY

It is challenging to retrieve pedestrians in the large spatio-temporal setting. In a larger space, there are more pedestrians with similar appearance, causing interference to retrieval. In the long-term span, the same person may change the clothes, leading to large appearance variation. The inter and intra-variations change much more significant than the short-term setting. This would result in a low mAP accuracy. Therefore, we aim to improve the mAP accuracy. In this section, we present a simple but effective method that directly optimizes the mAP value during training. Fig. 8 shows the flowchart of the framework. More details can be seen in the following sections.

A. Problem Formulation

Assume the query set is denoted as $\mathbb{Q} = \{q_i\}_{i=1}^{N_Q}$ and the gallery set is denoted as $\mathbb{G} = \{g_j\}_{j=1}^{N_G}$. Given a query person image $q_i \in \mathbb{Q}$, re-ID aims at retrieving the positive images with the same identity from the gallery \mathbb{G} . Most of the existing works learn a deep embedding network $f(x|\theta)$ that embeds x to a high dimensional Euclidean space. At the testing stage, each query $q_i \in \mathbb{Q}$ will return a ranking list of gallery \mathbb{G} , in which image g_j with closer Euclidean distance ranks higher. Finally, the mean average precision (mAP) is utilized to evaluate the ranking result. The mAP is the average AP (average precision) of all queries. AP refers to the area under the P-R curve composed of precision and recall. Therefore, the mAP can be represented as follows:

$$mAP = \frac{1}{N_Q} \sum_{i=1}^{N_Q} AP(i), \quad (1)$$

$$\begin{aligned} AP(i) &= \sum_{j=1}^{N_G} \left[P_i(j) \cdot \Delta R_i(j) \right], \\ &= \sum_{j=1}^{N_G} \left[P_i(j) \cdot (R_i(j) - R_i(j-1)) \right], \end{aligned} \quad (2)$$

where P and R denote the precision and recall value, respectively. N_Q and N_G denote the number of images in query and gallery sets. The final objective is shown as:

$$\begin{aligned} \min \quad & 1 - mAP(\mathbb{Q}, \mathbb{G}), \\ \text{s.t.} \quad & \mathbb{Q} = \{q_i\}_{i=1}^{N_Q}, \mathbb{G} = \{g_j\}_{j=1}^{N_G}. \end{aligned} \quad (3)$$

B. Learning Pipeline

The objective in the formula 3 is a discrete optimization problem. It involves the discrete sorting operation, which is difficult for gradient-based optimization. However, we can compute an approximation of mAP by using histograms [22–24]. The approximate version of mAP is differentiable. As shown in Fig. 8, our framework consists of metric learning[10] and the mAP optimization. More details are as follows.

Metric Learning. The cross-entropy loss \mathcal{L}_i and triplet loss \mathcal{L}_t are both used to optimize the embedding network. The losses can be denoted as follows:

$$\mathcal{L}_{metric} = \mathcal{L}_i + \mathcal{L}_t, \quad (4)$$

$$\mathcal{L}_i = \frac{1}{B} \sum_{i=1}^B \left(-y_i \cdot \log p(x_i) \right), \quad (5)$$

$$\mathcal{L}_t = \frac{1}{B} \sum_{i=1}^B \left(m + d_{max}(x_i, x_i^p) - d_{min}(x_i, x_i^n) \right), \quad (6)$$

where B is the batch size. x_i and y_i denote the input sample and its label, respectively. $p(x_i)$ is the predicted identity

probability. m is set 0.3. d_{max} and d_{min} denote the maximum distance of positive sample pairs and minimum distance of negative sample pairs.

The mAP optimization. Fig. 8 gives the whole pipeline of the mAP computation. To compute the mAP value, the AP value is computed for each query sample. Inspired by previous works [22, 23, 25, 26], we can use relaxation of AP by using a triangular kernel. As shown in Fig. 8, the pipeline of computing mAP is divided into several steps. First, we get the embeddings of samples. The length of the embedded features is 2048. All the features are normalized by L_2 norm. Then, we compute the cosine similarity $s_{ij} \in [-1, 1]$ of query $q_i \in \mathbb{Q}$ and gallery $g_j \in \mathbb{G}$. As the number of the gallery \mathbb{G} is $N_{\mathbb{G}}$, the similarity vector can be denoted as $\mathbf{s} = [s_{i1}, s_{i2}, \dots, s_{iN_{\mathbb{G}}}]$. Next, we sort \mathbf{s} and compute its histogram. Since the sorting operation is non-differentiable, a triangular kernel is used as an approximation and defined as follows:

$$\Delta(s_{ij}, m) = \max\left(1 - \frac{|s_{ij} - b_m|}{\varepsilon}, 0\right), \quad (7)$$

where b_m is the m -th bin of the histogram with a range of $[-1, 1]$. ε denotes the interval between adjacent bins. Assume the number of bins is M , then $\varepsilon = \frac{2}{M-1}$.

The triangular kernel consists of M triangles. The similarity vector \mathbf{s} is input into the triangular kernel. If the item s_{ij} is not in the interval of $[b_m - \varepsilon, b_m + \varepsilon]$, the output $\Delta(s_{ij}, m)$ would be set zero and the item s_{ij} would be removed. In this way, all the similarity items in \mathbf{s} are sorted and we get a ranking list of \mathbf{s} . After the above operations, all the items in \mathbf{s} are assigned into corresponding bins. Finally, the precision P and recall R in the formula (2) can be computed.

$$P_i(j) = \frac{\sum_{m=1}^j \sum_{n=1}^{N_{\mathbb{G}}} (\Delta(s_{in}, j) \cdot \bar{y}_{in})}{\sum_{m=1}^j \sum_{n=1}^{N_{\mathbb{G}}} (\Delta(s_{in}, j))}, \quad (8)$$

$$\Delta R_i(j) = \frac{\sum_{n=1}^{N_{\mathbb{G}}} (\Delta(s_{in}, j) \cdot \bar{y}_{in})}{\sum_{n=1}^{N_{\mathbb{G}}} (\bar{y}_{in})}, \quad (9)$$

where $\Delta R_i(j) = R_i(j) - R_i(j-1)$. s_{in} is the similarity between q_i and g_n . $\bar{y}_{in} \in \{0, 1\}$ indicates whether belongs to the same identity. The mAP loss can be denoted as:

$$\mathcal{L}_{mAP} = 1 - \frac{1}{N_{\mathbb{Q}}} \sum_{i=1}^{N_{\mathbb{Q}}} \sum_{j=1}^{N_{\mathbb{G}}} [P_i(j) \cdot \Delta R_i(j)]. \quad (10)$$

In summary, the overall loss functions can be formulated as follows:

$$\mathcal{L} = \mathcal{L}_{metric} + \mathcal{L}_{mAP}. \quad (11)$$

V. EXPERIMENTS

A. Implementation Details

1) *Datasets*: Three types of datasets are used in the following experiments: short-term datasets (Market1501 [5], DukeMTMC [6], and MSMT17 [13]), cloth-changing dataset (PRCC [7]), and spatio-temporal datasets (Celeb-reID [20], LaST).

TABLE II
STATISTICS OF TRAIN/VALIDATION/TEST SETS ON LAST.

Quantity	Train	Validation		Test	
		Query	Gallery	Query	Gallery
Identities	5000	56	57	5803	5805
Images	70,923	100	20,484	10,173	123,041

TABLE III
RE-ID RESULTS ON THE PROPOSED LAST DATASET.

Methods	Year	R1	R5	R10	R20	mAP
PCB[29]	2018	56.2	73.5	79.0	83.7	19.1
MGN[30]	2018	41.0	63.0	76.0	78.0	17.6
SFT[31]	2019	61.2	75.3	79.9	83.5	19.3
MHN[32]	2019	53.7	70.5	76.1	81.0	15.4
OSNet[33]	2019	63.8	78.2	82.6	85.9	20.9
ABD-Net[34]	2019	52.1	71.0	77.4	82.7	18.9
BDB[35]	2019	62.2	78.2	82.9	86.7	19.8
PyrNet[36]	2019	56.4	73.2	78.3	82.7	17.2
BoT[37]	2019	68.3	82.3	85.9	89.1	25.3
HPM[38]	2019	64.0	80.0	87.0	89.0	26.8
Top-DB-Net[39]	2020	69.4	82.8	86.3	89.3	25.0
HOREID[40]	2020	68.3	82.3	86.2	89.2	25.5
CtF[41]	2020	69.9	82.8	86.2	89.3	26.5
QAConv[42]	2020	64.6	82.4	79.3	83.5	22.4
Ours	2021	69.9	83.6	87.2	90.0	27.6

Market1501 [5] is a widely-used person re-ID dataset. It contains 32,668 images of 1,501 identities captured by 6 cameras. Among them, 12,185 images of 751 identities are used for training. 15,913 images of 750 identities are used for testing gallery and 3,368 images are testing query. DukeMTMC-reID [6] is captured by 8 cameras, which contains 36,411 images and 1,812 identities. MSMT [13] is a large-scale dataset, which contains 124,068 images and 4,101 identities. PRCC [7] is a cloth-changing dataset. It contains 221 identities and 33,698 images. Celeb-reID was acquired from the Internet using street snap-shots of celebrities. It contains 1,052 identities and 34,186 images.

LaST contains 10,860 identities and 224,721 images. As shown in Table II, it is split into a training set with 70,923 images, an evaluation set with 20,584 images, and a test set with 133,214 images. The identities are 5,000, 56 and 5,803, respectively.

2) *Experimental Setup*: We use ResNet50 [27] as the backbone network, which is initialized with ImageNet [28] pre-trained model. The input images are resized to 256×128 and augmented by random horizontal flip and random erasing. The dimension of the extracted features is 2048. The SGD optimizer is used in our experiments. The initial learning rate is 3.5×10^{-3} . The mini-batch size is 64, which contains 16 identities and 4 images for each identity.

3) *Evaluated Metrics*: We utilize the cumulative matching characteristic (CMC) curve and mean average precision (mAP) as evaluation metrics. CMC curve is a precision curve that provides recognition precision for each rank. mAP is the

TABLE IV
EVALUATION OF PROPOSED METHOD ON CLOTH-CHANGING AND UNREAL SCENE DATASETS.

Methods	PRCC		Celeb-reID	
	R1	mAP	R1	mAP
HACNN[43]	21.8	-	47.6	9.5
PCB[29]	22.9	-	37.1	8.2
SPT[7]	34.4	-	-	-
ReIDCaps[20]	-	-	51.2	9.8
Baseline[37]	50.7	49.8	52.3	9.2
Ours	57.5	54.7	54.4	11.8

TABLE V
ABLATION STUDIES OF OUR METHOD ON LaST. \mathcal{L}_{metric} DENOTES METRIC LEARNING. \mathcal{L}_{mAP} DENOTES THE MAP OPTIMIZATION.

\mathcal{L}_{metric}	\mathcal{L}_{mAP}	R1	R5	R10	R20	mAP
✓		68.3	82.3	85.9	89.1	25.3
	✓	65.1	79.8	84.0	87.5	24.0
✓	✓	69.9	83.6	87.2	90.0	27.6

average precision value across all queries, which is much more effective than CMC when multiple ground truth exist in the gallery.

B. Evaluation of Proposed Method

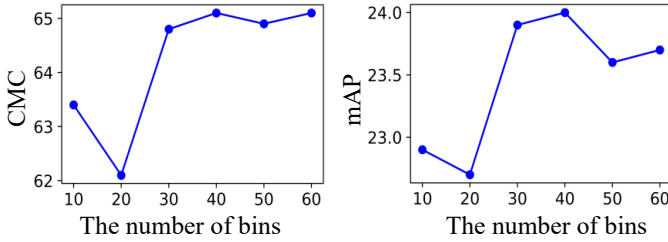


Fig. 9. The effect of histogram bins on final performance.

1) *Evaluation on LaST*: First, we evaluate 14 representative algorithms on LaST. These algorithms achieve superior performance on conventional datasets and their codes have been released on Github. To facilitate future comparison, we report Rank1, Rank5, Rank10, Rank20, and mAP accuracies. Table III shows us that the performances of existing methods are quite poor on LaST. For example, CtF [41] achieves 69.9% on Rank1 accuracy and 26.5% on mAP, which is the best among current methods. However, the mAP values of all algorithms are lower than 30%. This is due to the large visual variances induced by large spatial and temporal spans. For example, it is difficult to retrieve pedestrians when clothes have been changed. The experimental results demonstrate that LaST is a challenging benchmark so far. As shown in Table III, our method achieves 69.9% on Rank1 accuracy, which is the same as CtF. But our method achieves 27.6% on mAP, which surpasses most existing methods. This benefits from the mAP optimization, which directly optimizes the mAP value during training.

TABLE VI
PERFORMANCE COMPARISON OF DIRECT TRANSFER. THE MODEL WAS TRAINED AND TESTED ON DIFFERENT DATASETS.

Training Set	PRCC		Celeb-reID	
	R1	mAP	R1	mAP
ImageNet[28]	24.7	13.5	28.7	3.0
Market1501[5]	29.0	24.3	36.7	3.7
DukeMTMC[44]	28.3	24.1	40.9	4.6
MSMT17[13]	26.2	24.6	43.4	5.0
LaST	39.3	32.6	47.0	7.0

TABLE VII
PERFORMANCE COMPARISON OF DOMAIN ADAPTATION. THE MODEL WAS TRAINED AND TESTED ON PRCC AND CELEB-REID, RESPECTIVELY.

Pre-Training	PRCC		Celeb-reID	
	R1	mAP	R1	mAP
ImageNet[28]	43.1	43.1	49.2	8.7
Market1501[5]	44.3	43.1	49.3	8.7
DukeMTMC[44]	43.9	44.2	49.8	8.9
MSMT17[13]	43.7	44.1	51.0	9.0
LaST	54.4	54.3	56.1	11.7

2) *Evaluation on PRCC and Celeb-reID*: To verify the generalization ability of our method, we further conduct experiments on PRCC and Celeb-reID. PRCC [7] is a cloth-changing dataset and Celeb-reID [18] is a spatio-temporal dataset. We utilize BoT [37] as the baseline and compare it with our proposed method. As shown in Table IV, the performance of our method is much better than other methods. Compared with the baseline, ours boosts the mAP accuracy by 15.5% and 2.6% on PRCC and Celeb-reID, respectively. The above experiments demonstrate the effectiveness of our method.

C. Ablation Study

1) *Effectiveness of the mAP Optimization*: In Table V, we evaluate the metric learning and the mAP optimization, respectively. In the long-term setting, the appearance of the same person would change significantly. It is quite challenging to retrieve a person with large appearance variation. Therefore, the mAP value would be very poor. In this work, we focus on improving the mAP value. As shown in Table V, the mAP optimization still achieves 65.1% on Rank1 accuracy and 24.0% on mAP even only the mAP loss is used. The combination of metric learning and mAP optimization achieves the best performance. In other words, the mAP optimization has indeed promoted the final performance to some extent.

2) *The Effect of Histogram Bins*: The histogram is used to calculate the mAP value. To obtain the histogram, the interval $[-1, 1]$ is firstly split into M bins. Then the AP value is computed in each bin. As this method is an approximation of mAP, the number of bins will affect the accuracy of mAP calculation, and then affect the final performance. We conduct experiments on LaST and show the results in Fig. 9. It shows us that the Rank1 and mAP accuracies change with the number

TABLE VIII
PERFORMANCE COMPARISON ON SHORT-TERM DATASETS. THE MODEL WAS TRAINED AND TESTED ON MARKET1501 AND DUKEMTMC, RESPECTIVELY.

Pre-Training	Market1501		DukeMTMC	
	R1	mAP	R1	mAP
ImageNet[28]	89.0	71.1	78.7	62.8
MSMT17[13]	92.5	79.2	84.4	70.7
LaST	91.4	79.1	82.5	69.0
LaST_Cloth	93.1	81.7	84.5	71.7

TABLE IX
PERFORMANCE COMPARISON OF IDENTITY COMBINATION. THE TRAINING DATA CONTAINS THE TRAINING SET AND TARGET SET. THE MODEL WAS TESTED ON THE TARGET SET, *i.e.*, MARKET1501 AND DUKEMTMC.

Training Set	Market1501		DukeMTMC	
	R1	mAP	R1	mAP
+MSMT17[13]	91.7	77.4	83.4	69.7
+LaST_Cloth	92.3	80.0	84.3	70.2

of bins. Since they achieve the best when the bin number is 40, the bin number is set 40 in our approach.

D. Generalization of LaST on Cloth-changing Setting

1) *Direct Transfer Evaluation*: To evaluate the generalization ability of LaST, we first conduct direct transfer experiments. For example, we train the model on Market1501 and test it on PRCC dataset. In the following experiments, we utilize BoT[37] as the baseline method. As shown in Table VI, five large-scale datasets are used as the training sets. The two cloth-changing datasets, PRCC [7] and Celeb-reID [18], are used as the test sets. Although ImageNet has millions of images, its direct transfer performance is far inferior to other pedestrian-based datasets. This is because that most samples in ImageNet are not persons. Learning on pedestrian datasets are more helpful to learn discriminative human cues. Table VI shows LaST achieves the best performance. For example, it achieves the Rank1 accuracy of 39.3% on PRCC, 13.1% higher than MSMT17. This benefits from the larger diversity in LaST, leading to a better generalization performance.

2) *Domain Adaptation*: When a few labeled samples on target domains are available, domain adaptation can be simply done by supervised fine-tuning on the pre-trained model. For example, the model is firstly initialized with the pre-trained parameters on Market1501, then it is fine-tuned on PRCC dataset. As shown in Table VII, five datasets are used as the source datasets. The pre-trained models on the five datasets are utilized to initialize the backbone network. Then the network is trained and tested on the target domain. We can see that the performance of all datasets has been boosted to some extent. This is benefited from the source datasets. LaST achieves 54.4% and 56.1% on Rank1 accuracy, respectively. It surpasses all other datasets on two target domains. The above experiments fully demonstrate the superior generalization ability of LaST on cloth-changing scenarios.

E. Generalization of LaST on Short-term Setting

1) *Performance Comparison*: Although LaST is designed for large-scale spatio-temporal person re-ID, we are still interested in its generalization ability in the short-term setting. Since MSMT17 is much larger than Market1501 and DukeMTMC, we utilize it as the pre-training dataset. For example, the model is firstly initialized with the parameters pre-trained on MSMT17, then it is trained and tested on Market1501 and DukeMTMC.

Table VIII shows us that the performance of LaST is better than ImageNet but still poorer than MSMT17. This is because that the task of large-scale spatio-temporal person re-ID is different from conventional short-term person re-ID task. **In the short-term setting, pedestrians would not change their clothes and clothing cues are enough discriminative. However, clothing cues may not be reliable in the large-scale spatio-temporal settings.** The model trained with LaST mainly focuses on cloth-irrelevant cues. The lack of clothing features leads to the loss of generalization performance on short-term re-ID datasets. Therefore, the performance of LaST is poorer than MSMT17.

2) *Cloth-based Pre-training Strategy*: Based on the above analysis, we proposed a new pre-training strategy for the short-term setting. Each person in LaST may have several clothes. As shown in Fig. 7, we regard the samples with different clothes as different labels, even they belong to the same person. **The traditional training methods use pedestrian ID as the label, but our new pre-training strategy utilizes clothes as the label.** We denote the new pre-training strategy as “LaST_Cloth”. As shown in Table VIII, it significantly boosts the generalization performance and achieves the Rank1 accuracy of 93.1% and 84.5% on Market1501 and DukeMTMC, respectively. These experiments demonstrate the effectiveness of our new pre-training strategy. Therefore, we could utilize pedestrian labels for the cloth-changing setting and clothing labels for the short-term setting. This benefits from the dense annotation of clothes. LaST is the only person re-ID data set to label clothes at present.

3) *Evaluation on Identity Combination*: To further verify the effectiveness of the proposed cloth-based training strategy, we conducted the identity combination experiments in Table IX. For example, we combine MSMT17 and Market1501 as the training set. Since their identity numbers of training sets are 1,041 and 751, respectively, the total identity number of the combined dataset becomes 1,792. Then we train the combined dataset and evaluate the test set of Market1501. Table IX shows us that “+LaST_Cloth” still achieves better performance in both Market1501 and DukeMTMC. This further demonstrates the effectiveness of the cloth-based training strategy in short-term person re-identification.

F. Visualization

To verify the correctness of the above analysis, we visualize the heat maps in Fig. 10. The class activation mapping (CAM) [45] is used to generate the heat maps. The brighter the pixels are, the more attention the model pays to.

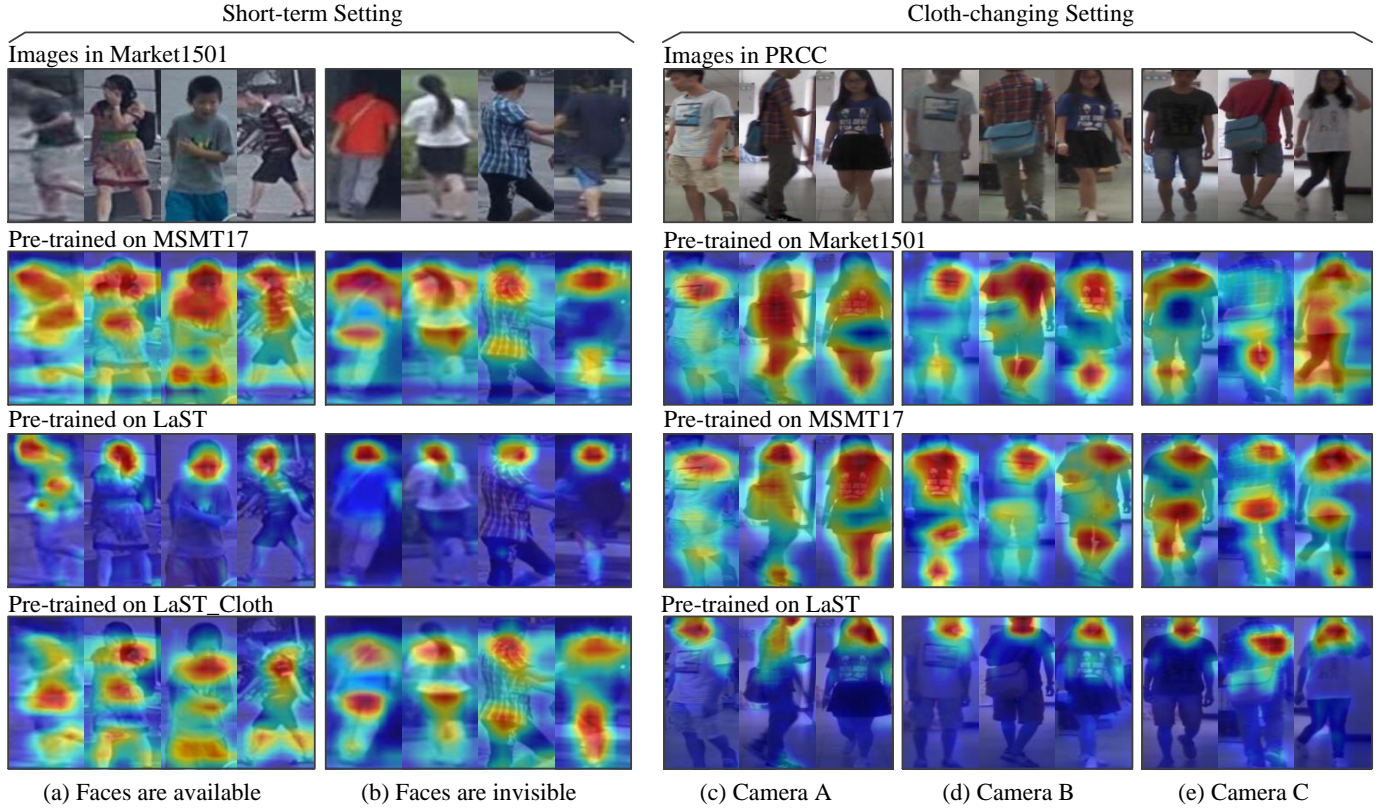


Fig. 10. **The visualization of heat maps calculated by different pre-trained models.** For example, “Pre-trained on MSMT17” means that the model is firstly trained on MSMT17. Then the trained model is used to visualize the images in Market1501.

1) *Short-term Setting*: We utilize three pre-trained models to visualize the heat maps on Market1501. As shown in Fig. 10(a), the model trained with LaST mainly focuses on the heads and ignores the clothing cues. Since clothing cues are quite discriminative in the short-term setting, ignoring them would lead to poor performance. Benefit from the cloth-based pre-training strategy, LaST_Cloth could focus on the clothes beside the head cues. This further demonstrates the effectiveness of the proposed pre-training strategy. Fig. 10(b) shows some instances when faces are invisible. It shows us that the model trained with LaST could still focus on the head, especially the hair.

We further give an illustration in Fig. 11. In the short-term setting, the similarity of pre-trained on MSMT17 is much larger than that of pre-trained on LaST. This is because more clothing cues with high similarity can be exploited. The model pre-trained on LaST mainly focus on the head. As the area of head pixel is small, the similarity of the head is smaller than that of clothing cues. However, the model pre-trained on LaST_Cloth could still learn clothing parts and achieve high match performance. The above visualizations fully explain why LaST behaves poorly in the short-term settings, while LaST_Cloth and MSMT17 have better generalization performance in this scenario.

2) *Cloth-changing Setting*: Fig. 10(c),(d) and (e) shows the visualization results on PRCC dataset. The pedestrians in camera A and B have the same clothes, but different from camera C. We could see that the models trained with Market1501

and MSMT17 still focus on the clothes even the clothes have been changed. This leads to their poor performance in cloth-changing settings. However, the model trained with LaST mainly focuses on the heads, which are more robust than clothes in this scenario. As shown in Fig. 11, the similarity values of clothing cues are small because the boy has changed his clothes. As the clothing cues are not still reliable, the learned clothing cues would deteriorate the performance. The similarity of pre-trained on MSMT is smaller than that of pre-trained on LaST. Therefore, LaST has a better generalization ability than Market1501 and DukeMTMC in cloth-changing settings.

G. Limitation and Discussion

The performance of person re-ID on short-term datasets is satisfied, but it has not been widely used in real applications to date. A partial reason is its not robust performance in the large-scale spatio-temporal scenes. This task has not been well studied because of a lack of datasets. In this work, we provide LaST to do research in this scenario. Pedestrians in LaST have large spatio-temporal spans. This provides many challenging problems. For example, some pedestrians appear both daytime and night, and some frequently change their clothes. Besides, LaST provides sufficient diversity in terms of pedestrians, clothes, age, scenes, and weather, *etc.* The experiments show us that most current methods achieve unsatisfied performance on LaST, especially the poor mAP value. To solve the problem, more discriminative cues need to be studied. For example,

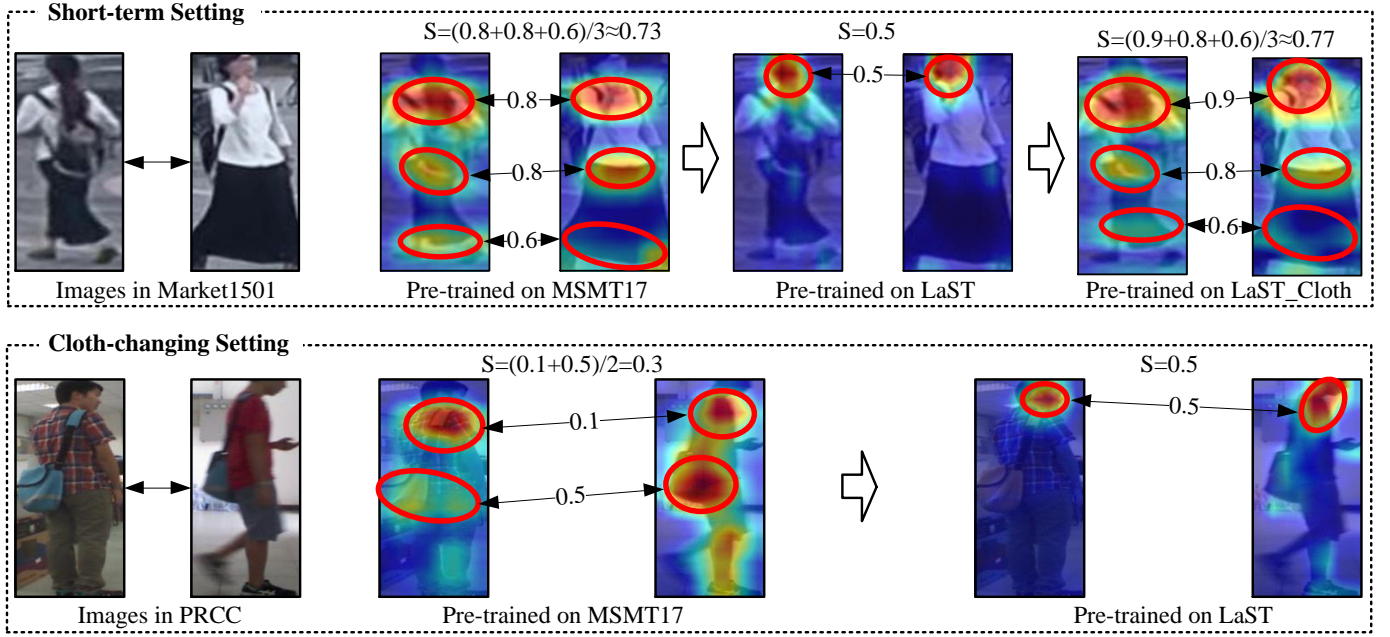


Fig. 11. **Similarity matching of learned parts among pre-trained models.** ‘S’ denotes the similarity value. As more clothing cues can be used, the similarity values of pre-trained on MSMT17 and LaST_Cloth are larger than that of pre-trained on LaST in the short-term setting. However, the learned clothing cues would deteriorate the performance in the cloth-changing setting. Therefore, the similarity value of pre-trained on MSMT17 is smaller than that of pre-trained on LaST.

the combination of body shape and discriminative appearance cues. This needs to be explored in the future.

VI. CONCLUSIONS

In this work, we study the large-scale spatio-temporal person re-identification. This task has much larger spatial and temporal spans than previous settings. Our major contribution is the large-scale benchmark dataset called LaST. It is the largest densely annotated re-ID benchmark and the first one to label clothes to date. By careful collection, the style of LaST is very similar to conventional re-ID datasets. Besides, we propose a simple but effective baseline that works well on such challenging person re-ID setting. Specifically, we directly optimize the mAP during training and achieve competitive performance compared with current methods. By conducting extensive experiments, we demonstrate that LaST has good generalization ability in both short-term and cloth-changing scenarios. We believe that there is still much room for improvement in the large-scale spatio-temporal settings. By releasing LaST, we expect this dataset to catalyze research in the re-ID community and propel the maturation of re-ID techniques in real-world applications.

REFERENCES

- [1] X. Jia, H. Zhao, Z. Lin, A. Kale, and V. Kumar, “Personalized image retrieval with sparse graph representation learning,” in *Proceedings of the ACM SIGKDD International Conference on Knowledge Discovery & Data Mining*, 2020, pp. 2735–2743.
- [2] J.-T. Huang, A. Sharma, S. Sun, L. Xia, D. Zhang, P. Pronin, J. Padmanabhan, G. Ottaviano, and L. Yang, “Embedding-based retrieval in facebook search,” in *Proceedings of the ACM SIGKDD International Conference on Knowledge Discovery & Data Mining*, 2020, pp. 2553–2561.
- [3] M. Ye, J. Shen, G. Lin, T. Xiang, L. Shao, and S. C. H. Hoi, “Deep learning for person re-identification: A survey and outlook,” *IEEE Transactions on Pattern Analysis and Machine Intelligence*, 2021.
- [4] W. Li, R. Zhao, T. Xiao, and X. G. Wang, “Deep-reid: Deep filter pairing neural network for person re-identification,” in *Proceedings of the IEEE/CVF Conference on Computer Vision and Pattern Recognition (CVPR)*, 2014, pp. 152–159.
- [5] L. Zheng, L. Shen, L. Tian, S. Wang, J. Wang, and Q. Tian, “Scalable person re-identification: A benchmark,” in *IEEE/CVF International Conference on Computer Vision (ICCV)*, 2015, pp. 1116–1124.
- [6] E. Ristani, F. Solera, R. S. Zou, R. Cucchiara, and C. Tomasi, “Performance measures and a data set for multi-target, multi-camera tracking,” in *ECCVW*, 2016, pp. 17–35.
- [7] Q. Yang, A. Wu, and W. S. Zheng, “Person re-identification by contour sketch under moderate clothing change,” *IEEE Transactions on Pattern Analysis and Machine Intelligence*, 2019.
- [8] S. Yu, S. Li, D. Chen, R. Zhao, J. Yan, and Y. Qiao, “Cocas: A large-scale clothes changing person dataset for re-identification,” in *Proceedings of the IEEE/CVF Conference on Computer Vision and Pattern Recognition (CVPR)*, 2020, pp. 3400–3409.
- [9] F. Wan, Y. Wu, X. Qian, Y. Chen, and Y. Fu, “When person re-identification meets changing clothes,” in

- IEEE/CVF Conference on Computer Vision and Pattern Recognition Workshops (CVPRW)*, 2019, pp. 3620–3628.
- [10] J. Wang, Y. Song, T. Leung, C. Rosenberg, and Y. Wu, “Learning fine-grained image similarity with deep ranking,” in *Proceedings of the IEEE/CVF Conference on Computer Vision and Pattern Recognition (CVPR)*, 2014, pp. 1386–1393.
 - [11] C. C. Loy, C. Liu, and S. Gong, “Person re-identification by manifold ranking,” in *IEEE International Conference on Image Processing (ICIP)*, 2014, pp. 3567–3571.
 - [12] W. Li, R. Zhao, and X. Wang, “Human reidentification with transferred metric learning,” in *Proceedings of the Asian Conference on Computer Vision (ACCV)*, 2012, pp. 31–44.
 - [13] L. Wei, S. Zhang, W. Gao, and Q. Tian, “Person transfer gan to bridge domain gap for person re-identification,” in *Proceedings of the IEEE/CVF Conference on Computer Vision and Pattern Recognition (CVPR)*, 2018, pp. 79–88.
 - [14] X. Qian, W. Wang, L. Zhang, F. Zhu, Y. Fu, T. Xiang, Y.-G. Jiang, and X. Xue, “Long-term cloth-changing person re-identification,” in *Proceedings of the Asian Conference on Computer Vision (ACCV)*, 2020.
 - [15] N. Zhang, M. Paluri, Y. Taigman, R. Fergus, and L. Bourdev, “Beyond frontal faces: Improving person recognition using multiple cues,” in *Proceedings of the IEEE/CVF Conference on Computer Vision and Pattern Recognition (CVPR)*, 2015, pp. 4804–4813.
 - [16] Q. Huang, Y. Xiong, and D. Lin, “Unifying identification and context learning for person recognition,” in *Proceedings of the IEEE/CVF Conference on Computer Vision and Pattern Recognition (CVPR)*, 2018, pp. 2217–2225.
 - [17] T. Xiao, S. Li, B. Wang, L. Lin, and X. Wang, “Joint detection and identification feature learning for person search,” in *Proceedings of the IEEE/CVF Conference on Computer Vision and Pattern Recognition (CVPR)*, 2017, pp. 3415–3424.
 - [18] Y. Huang, J. Xu, Q. Wu, Y. Zhong, P. Zhang, and Z. Zhang, “Beyond scalar neuron: Adopting vector-neuron capsules for long-term person re-identification,” *IEEE Transactions on Circuits and Systems for Video Technology*, vol. 30, no. 10, pp. 3459–3471, 2019.
 - [19] D. Gray and H. Tao, “Viewpoint invariant pedestrian recognition with an ensemble of localized features,” in *Proceedings of the European Conference on Computer Vision (ECCV)*, 2008, pp. 262–275.
 - [20] Y. Huang, J. Xu, Q. Wu, Y. Zhong, and Z. Zhang, “Beyond scalar neuron: Adopting vector-neuron capsules for long-term person re-identification,” *IEEE Transactions on Circuits and Systems for Video Technology*, vol. 30, no. 10, pp. 3459–3471, 2020.
 - [21] X. Zhang, F. Wan, C. Liu, R. Ji, and Q. Ye, “Freeanchor: Learning to match anchors for visual object detection,” in *Advances in neural information processing systems (NeurIPS)*, 2019, pp. 147–155.
 - [22] E. Ustinova and V. S. Lempitsky, “Learning deep embeddings with histogram loss,” in *Advances in neural information processing systems (NeurIPS)*, 2016, pp. 4170–4178.
 - [23] K. He, F. Cakir, S. A. Bargal, and S. Sclaroff, “Hashing as tie-aware learning to rank,” in *Proceedings of the IEEE/CVF Conference on Computer Vision and Pattern Recognition (CVPR)*, 2018, pp. 4023–4032.
 - [24] A. Brown, W. Xie, V. Kalogeiton, and A. Zisserman, “Smooth-ap: Smoothing the path towards large-scale image retrieval,” in *Proceedings of the European Conference on Computer Vision (ECCV)*, 2020, pp. 677–694.
 - [25] K. He, Y. Lu, and S. Sclaroff, “Local descriptors optimized for average precision,” in *Proceedings of the IEEE/CVF Conference on Computer Vision and Pattern Recognition (CVPR)*, 2018, pp. 4023–4032.
 - [26] J. Revaud, J. Almazan, R. S. De Rezende, and C. R. De Souza, “Learning with average precision: Training image retrieval with a listwise loss,” in *IEEE/CVF International Conference on Computer Vision (ICCV)*, 2019, pp. 5106–5115.
 - [27] K. He, X. Zhang, S. Ren, and J. Sun, “Deep residual learning for image recognition,” in *Proceedings of the IEEE/CVF Conference on Computer Vision and Pattern Recognition (CVPR)*, 2016, pp. 770–778.
 - [28] O. Russakovsky, J. Deng, H. Su, J. Krause, S. Satheesh, S. Ma, Z. Huang, A. Karpathy, A. Khosla, M. S. Bernstein *et al.*, “Imagenet large scale visual recognition challenge,” *International Journal of Computer Vision*, vol. 115, no. 3, pp. 211–252, 2015.
 - [29] Y. Sun, L. Zheng, Y. Yang, Q. Tian, and S. Wang, “Beyond part models: Person retrieval with refined part pooling (and a strong convolutional baseline),” in *Proceedings of the European Conference on Computer Vision (ECCV)*, 2018, pp. 501–518.
 - [30] G. Wang, Y. Yuan, X. Chen, J. Li, and X. Zhou, “Learning discriminative features with multiple granularities for person re-identification,” in *ACM Multimedia*, 2018, pp. 274–282.
 - [31] C. Luo, Y. Chen, N. Wang, and Z. Zhang, “Spectral feature transformation for person re-identification,” in *IEEE/CVF International Conference on Computer Vision (ICCV)*, 2019, pp. 4975–4984.
 - [32] B. Chen, W. Deng, and J. Hu, “Mixed high-order attention network for person re-identification,” in *IEEE/CVF International Conference on Computer Vision (ICCV)*, 2019, pp. 371–381.
 - [33] K. Zhou, Y. Yang, A. Cavallaro, and T. Xiang, “Omni-scale feature learning for person re-identification,” in *2019 IEEE/CVF International Conference on Computer Vision (ICCV)*, 2019, pp. 3701–3711.
 - [34] C. Tianlong, D. Shaojin, X. Jingyi, Y. Ye, C. Wuyang, Y. Yang, R. Zhou, and W. Zhangyang, “Abd-net: Attentive but diverse person re-identification,” in *IEEE/CVF International Conference on Computer Vision (ICCV)*, 2019, pp. 8350–8360.
 - [35] Z. Dai, M. Chen, X. Gu, S. Zhu, and P. Tan, “Batch drop-block network for person re-identification and beyond,” in *IEEE/CVF International Conference on Computer Vision (ICCV)*, 2019, pp. 3690–3700.
 - [36] N. Martinel, G. L. Foresti, and C. Micheloni, “Aggre-

- gating deep pyramidal representations for person re-identification,” in *IEEE/CVF Conference on Computer Vision and Pattern Recognition Workshops (CVPRW)*, 2019, pp. 1544–1554.
- [37] H. Luo, Y. Gu, X. Liao, S. Lai, and W. Jiang, “Bag of tricks and a strong baseline for deep person re-identification,” in *IEEE/CVF Conference on Computer Vision and Pattern Recognition Workshops (CVPRW)*, 2019, pp. 1487–1495.
- [38] Y. Fu, Y. Wei, Y. Zhou, H. Shi, G. Huang, X. Wang, Z. Yao, and T. Huang, “Horizontal pyramid matching for person re-identification,” in *Proceedings of the Proceedings of the AAAI Conference on Artificial Intelligence (AAAI) Conference on Artificial Intelligence*, vol. 33, no. 01, 2019, pp. 8295–8302.
- [39] R. Quispe and H. Pedrini, “Top-db-net: Top dropblock for activation enhancement in person re-identification,” in *International Conference on Pattern Recognition (ICPR)*, 2020.
- [40] G. Wang, S. Yang, H. Liu, Z. Wang, Y. Yang, S. Wang, G. Yu, E. Zhou, and J. Sun, “High-order information matters: Learning relation and topology for occluded person re-identification,” in *Proceedings of the IEEE/CVF Conference on Computer Vision and Pattern Recognition (CVPR)*, 2020, pp. 6448–6457.
- [41] G. Wang, S. Gong, J. Cheng, and Z. Hou, “Faster person re-identification,” in *Proceedings of the European Conference on Computer Vision (ECCV)*, 2020, pp. 275–292.
- [42] S. Liao and L. Shao, “Interpretable and generalizable person re-identification with query-adaptive convolution and temporal lifting,” in *Proceedings of the European Conference on Computer Vision (ECCV)*, 2020, pp. 456–474.
- [43] W. Li, X. Zhu, and S. Gong, “Harmonious attention network for person re-identification,” in *Proceedings of the IEEE/CVF Conference on Computer Vision and Pattern Recognition (CVPR)*, 2018, pp. 2285–2294.
- [44] Z. Zheng, L. Zheng, and Y. Yang, “Unlabeled samples generated by gan improve the person re-identification baseline in vitro,” in *IEEE/CVF International Conference on Computer Vision (ICCV)*, 2017, pp. 3754–3762.
- [45] B. Zhou, A. Khosla, A. Lapedriza, A. Oliva, and A. Torralba, “Learning deep features for discriminative localization,” in *Proceedings of the IEEE/CVF Conference on Computer Vision and Pattern Recognition (CVPR)*, 2016, pp. 2921–2929.